Engineering and Technology Journal
Journal homepage: https://etj.uotechnology.edu.iq

Artificial Neural Network-Based Transmission Power Control for Underwater Wireless Optical Communication System

Omar N. Mohammed Salim [a,b], **Salah A. Adnan** [a*], **Ammar H. Mutlag** [b]

[a] Laser and Optoelectronics Engineering Dept., University of Technology-Iraq, Alsina'a street, 10066 Baghdad, Iraq.
[b] Electrical Engineering Technical College, Middle Technical University- Baghdad, Iraq
*Corresponding author Email: salahaldeen.a.taha@uotechnology.edu.iq

HIGHLIGHTS

- A 450 nm Underwater Wireless Optical Communication System was implemented in this study.
- Bit error rate was measured in the tap water channel for 2Mbit/s,10Mbit/s, and 20Mbit/s.
- The optimization for striking a balance between low power consumption and reliable data transfer in underwater ambient was investigated.
- A FFBP-ANN model-based transmission power control for the UWOC system has been adopted.
- power needed in multiple scenarios.

ARTICLE INFO

Handling editor: Evan T. Salim

Keywords:
UWOC; ANN; transmitted power control; neural network; back-propagation algorithm.

ABSTRACT

Underwater wireless optical communication systems (UWOC) have been proposed as a means of delivering high-speed data services while utilizing the abundant optical spectrum. However, when using undersea channels, wireless optical signal propagation faces an antagonistic environment due to factors such as scattering, absorption, turbulence, and optical link misalignment between the transmitter and the receiver. These factors will deteriorate the optical signal and lessen system performance. To mitigate the impact of these factors on communication system performance, transmitted optical power (OTP) should be increased. Since the UWOC system is battery-powered, increasing OTP will need more electricity. As a result, OTP must always be adjusted to reflect the changes there in the underwater channel. Therefore, an ANN model for link adaptation is proposed in this article, which can adjust the OTP level in tandem with the underwater channel conditions. Tap water was used as a transmission medium to collect data for training, testing, and validation of the proposed system reliability. The proposed model's output demonstrates that reliable performance in predicting OTP required in multiple scenarios is achieved. In the training, testing, and validation stages, the MSE of the predicted OTP is (9.510^{-3}, 1.510^{-2}, and 1.710^{-2}) dBm, respectively. The regression coefficients of the training, testing, and validation sets are calculated (0.9997,0.9990, and 0.9996). The proposed model's results demonstrate that it is reliable for use in UWOC systems.

1. Introduction

A growing number of undersea applications, such as oceanographic studies, ocean environment monitoring, oil and mineral exploration, and military requirements, place an increased burden on communication technologies [1,2]. As a result, Underwater Wireless Optical Communication (UWOC) has recently attracted a lot of attention as an appropriate and effective transmission option for a wide assortment of underwater applications [3]. Underwater acoustic communication (UWOC) has a lower bandwidth, speed, and security than Wireless Optical Communication (WOC), which has a lower time delay and larger bandwidth, making it more suitable for the underwater ecosystem [4]. The aforementioned advantages have prompted UWOC research to become more in-depth in recent years [5]. Because of the absorption, scattering, and turbulence of UWOC channels, optical beams will be hampered [6]. Due to channel deterioration, this would result in a significant reduction in optical signal strength for underwater broadcasts [7]. To evaluate the complex UWOC channel conditions, research has been done to model the effects of turbulence, scattering, and absorption for a fairly precise channel model [8]. For the modelling of UWOC channels, a Monte Carlo simulation, a future optimization algorithm, and a radiative transfer approach have been presented [9, 10]. Most

http://doi.org/10.30684/etj.2022.136247.1309
Received 15 October 2022; Accepted 25 December 2022; Available online 28 January 2023
2412-0758/University of Technology-Iraq, Baghdad, Iraq

UWOC studies assume that the transmitter and receiver are perfectly aligned. Unfortunately, due to vacillation and sea wave movements, it is difficult to meet this requirement in practical systems [8].

Many neural network (NN) models have been proposed as solutions to challenges in UWOC channel detection, estimation, and classification in recent years [11, 12]. These model scenarios, however, are limited to the lab-controlled environment with fixed inherent and apparent optical properties. In a real underwater environment, optical properties are constantly changing due to the unpredictable deviations caused by waterbody fluctuations [2, 6]. As a direct consequence, the practical UWOC devices' performance will be limited and static. Because UWOC equipment maintenance is a complicated process, UWOC transmitters and receivers are battery-powered devices. As a result, being aware of the specific optical transmission power (OTP) for a particular underwater communication channel is critical for conserving energy and extending the life of equipment and batteries. Some studies examined techniques for conserving and controlling power in underwater communication systems, with the majority focusing on acoustic systems [13]. Combining acoustic-optical communication is one technique used to save and control power transmitted in underwater communication systems [14]. The main idea behind this technique is a hybrid of multi-modal underwater communication techniques that complement and compensate for one another's flaws [15]. Artificial neural networks (ANN) are now designed to solve a wide range of scientific problems [16, 17]. The applications of NN, which fall into four major categories: prediction, control, pattern recognition, and optimization [18, 19], address real-world problems ranging from economics to geology. Researchers in the field of artificial intelligence are responsible for a plethora of recent achievements, including those in robotics, voice and image recognition, and the use of ANNs in real-world systems [20, 21]. The ANN system is based on mathematics and computations that mimic human brain processes [22]. Each of the ANN models has its layout format. ANN's architecture is based on the architecture of a biological system [23]. The neurons in ANN models are organized in a nonlinear and complex manner [22]. Individual neurons are linked using weighted links [24, 25]. Training and learning methods are used to compute all of the processes involved in ANN models, such as data collection and analysis, weights and biasing trade-offs, network structure design, and network simulation [19, 26]. The effectiveness of an ANN model is largely determined by its architecture, where the algorithm used for training and the structure chosen during the training process are critical factors in ANN performance [27, 28]. Many other optimization algorithms, such as adaptive neural-fuzzy inference, could be combined with the ANN model [29].

ANN model was proposed in this work to fulfil a dynamic UWOC system. The main contribution of this article is that the proposed system will be capable of setting a proper level for transmitted power based on the conditions of the underwater optical channel. The experimental study's configuration will be described and explained in the subsequent section. In the third section, the structure of the adopted ANN model will be shown. The fourth section will present and discuss the results, and the fifth section will draw article conclusions.

2. Experimental Study

The proposed UWOC System's experimental configuration was carried out in a water tank with dimensions of 8 m 1.25 m 1 m. Tap water was used to fill the tank. The proposed experimental block diagram of the laser UWOC system with on-off-keying non-return to zero (OOK-NRZ) modulation is shown in Figure 1. A 4.2 GHz wideband bias-tee is used to combine direct current (DC) from the power supply with a 211-1 PRBS from an arbitrary waveform generator (AWG). The combined signal is then supplied by the bias-tee to a laser diode (LD) of (450 nm, 1500 mW). The built optical transmitter sends modulated OOK-NRZ optical signals through the underwater channel. The employed silicon photomultiplier (SiPM) detector will convert the optical signal transmitted through an underwater channel to an electrical signal (ONSEMI MICROFC-30035). The optical signal emitted by LD illuminated the SiPM. The SiPM sensor's electrical signal will be sent to the oscilloscope (OSC) and computer for processing and data acquisition.

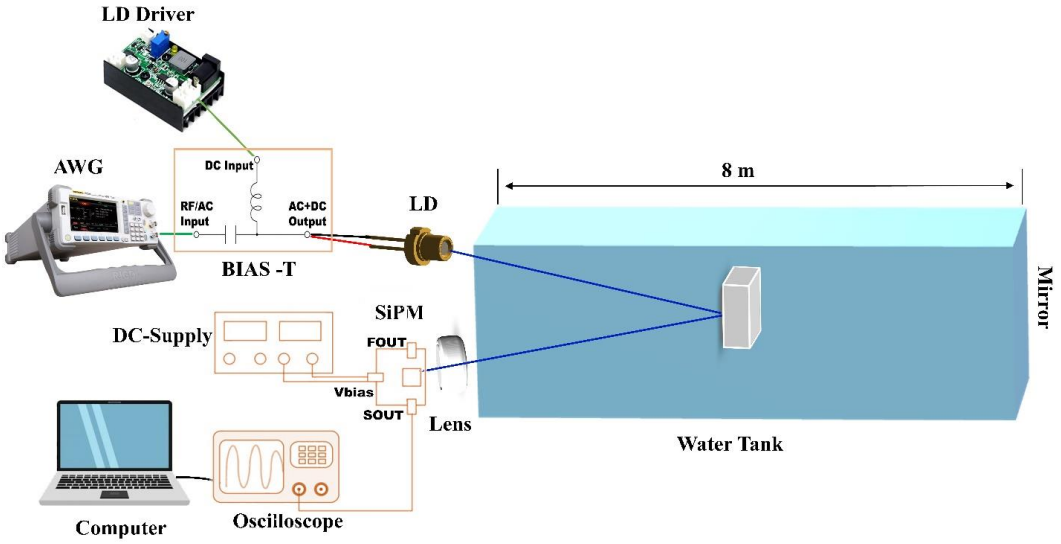

Figure 1: Experimental system schematic

Since the UWOC system operates in a volatile environment and system equipment is powered by a battery, controlling OTP is critical for optimizing UWOC system performance. As a consequence, automatic channel adaptation is required to allow the transmitter to adjust its transmission settings to the actual channel conditions. The most efficient method for adapting a communication channel is by far feedback from the receiver. Equation 1 describes the optical signal received by the SiPM:

$$\mathcal{S} = \mathcal{R} * h * S + n_d \quad (1)$$

Where the $\mathcal{R}$, h, and S denotes SiPM responsivity, channel status coefficient, and modulated transmitted optical signal, respectively. The symbol n_d represents the noise of the SiPM detector. The total effects and attenuation of the water channel are represented by the channel status coefficient h described by Equation 2:

$$h = \frac{ORP}{OTP} \quad (2)$$

Where the ORP is the optical received power. According to Eq. 1 and 2 the performance of the UWOC system is strongly dependent on the channel status.

Based on the current channel conditions, future transmission power levels could be predicted using the bit error rate BER, distance from the transmitter, and transmitted data rate. To adopt the new OTP level, this data is sent back to the transmitter via a feedback channel. The BER for signals passing through an underwater channel was explored in the experimental study for multiple bitrates/sec and OTP levels. The data collected from various transmission cases in the underwater channel was then used to train the ANN system to predict the best OTP. The transmitter should use this OTP, as shown in Figures 2 and 3. Figure 2 depicts the BER against channel distance of a 450 nm laser transmission in a tab water channel without turbulence for three different transmitting powers (24, 26, and 27 dBm), where 2-a represents the signal transmitted at a data rate of 2 Mbit/s, 2-b denotes the signal transmitted at a data rate of 10 Mbit/s, and 2-c reflects the signal transmitted at a data rate of 20 Mbit/s. Figure 3 depicts the BER against channel distance with a turbulent tap water channel for three different transmitted powers (24, 26, and 27 dBm). In 3-a, the signal is transmitted at a data rate of 2 Mbit/s, in 3-b, the signal is transmitted at a data rate of 10 Mbit/s, and in 3-c, the signal is transmitted at a data rate of 20 Mbit/s.

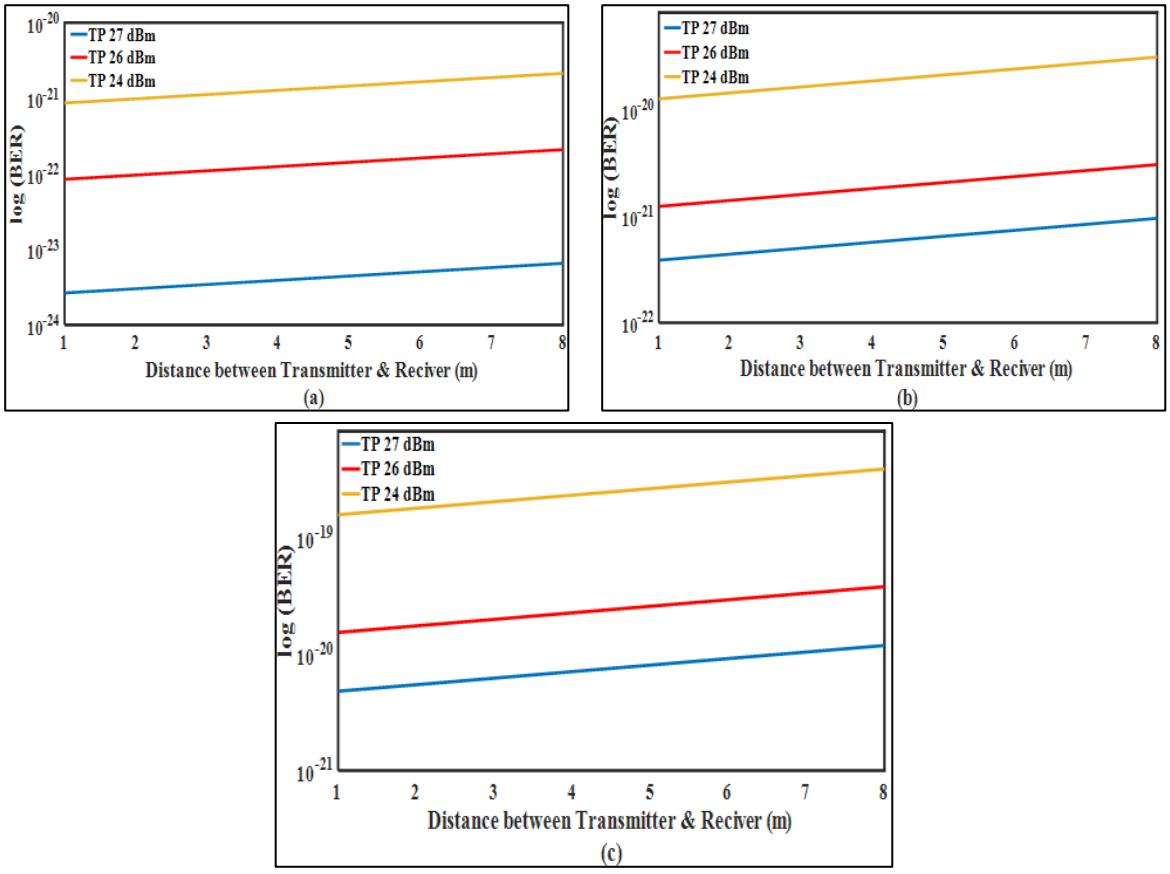

Figure 2: BER vs. Distance of transmission for tap water channel without turbulence (a) at 2Mbit/s (b) at 10Mbit/s (c) at 20Mbit/s

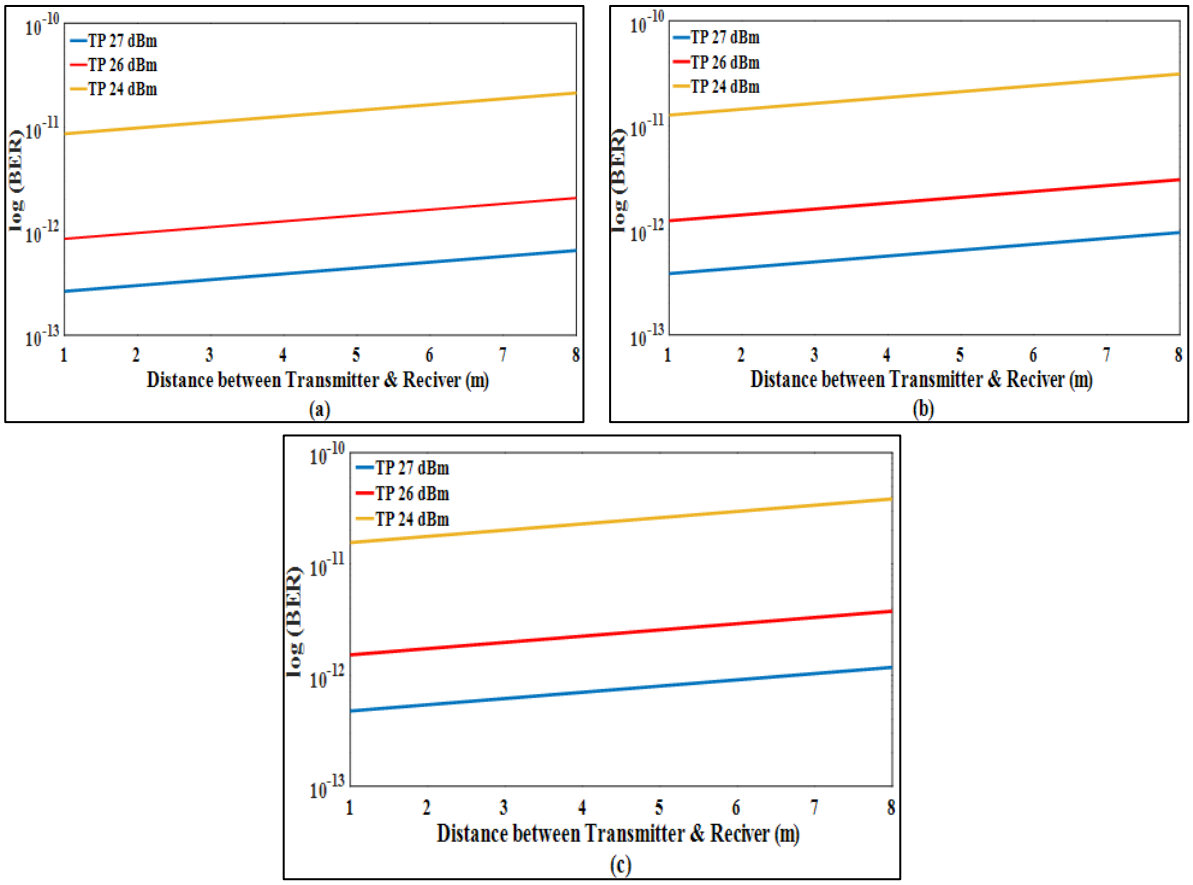

Figure 3: BER vs. Distance of transmission for tap water channel with turbulence (a) at 2Mbit/s (b) at 10Mbit/s (c) at 20Mbit/s

3. Structure of The Adopted ANN

Neural networks are computational approaches that can be harnessed for information processing, machine learning, and anticipating composite system responses based on previously learned information [30]. Over the past few years, there have been breakthroughs in the application of artificial NNs [31]. An artificial NN mimics the activities of the brain [32]. Training and data carrying can optimize synapses that connect neurons [22]. A variety of training approaches have been employed to create an artificial NN [33]. Six of the most well-known NN training methods have been tested in this article to pick the optimum one to use in the proposed system.

The feed-forward (FF) back-propagation (BP) neural network was the first to be tested. Mean squared error (MSE) and gradient descent (GD) have been used in this algorithm to modify the weight of network connections [34]. The connection weight is being adjusted in an attempt to reduce the network's error sum [19]. To begin, the network's connection value is given a low value, and then a training sample is chosen to calculate the gradient of error in comparison to that sample [35]. The weight of the connection is being altered in an attempt to reduce the network's error sum [36]. In the beginning, a limited value is assigned to the network's connection value, and a training sample is elected to compute the gradient of error proportionally to the sample [37]. The input signal is transmitted from the input layer to the output layer via the hidden layer during the forwarding propagation of the operational signal [38]. If the weight and offset values of each layer of a neuron are kept constant during forwarding propagation, their status only affects the next layer's status [34]. If the output layer fails to meet expectations, the BP of the error may be used [19]. The error signal is the discrepancy between the network's actual output and the expected output [22]. The error signal propagates layer by layer from the network's output layer end to the input layer in the BP method, and the weight of the network is modified by error feedback [33]. The weight and offset values are constantly changed to ensure that the network's output is as consistent with the expected one as possible [37].

The cascade forward (CFD) neural network was tested after the BP NN. In the CFD method, there are more weight connections between layers than that in FF networks, whereas, in CFD-NN, weight connections can be seen from the input layer to each layer in the network [39]. While a two-layer FF network can be trained in almost any input-output relationship, FF networks with additional layers may be able to learn more complicated relationships faster [40]. To clarify, if we spouse that we have three-layer networks, it will have connections between layers 1 and 2, layers 2 and 3, and layers 1 and 3. The ability of the network to learn the required relationship may be improved by adding more connections [39]. The BP method, such as the FF-BP method, is used to update the weights in the CFD artificial intelligence model, with the addition that each layer of neurons is related to all preceding layers of neurons.

Elman (ELM) neural network was the third NN that was tested. ELM-NN is a feedback NN that is optimized based on Elman's BP-NN research. In ELM-NN, a hidden layer adds an undertaking layer based on the BP algorithm that is used to store time delays, enabling the NN system to be adjusted with varying dynamic characteristics over time and also to achieve potent global stability [41]. There seem to be four layers in the ELM-NN structure: input, hidden, undertaking, and output [41]. When the undertake layer is used to remember hidden layer outputs, it is viewed as a delay operator for the steps. The delay and storage of the undertaking layer, which is based on the BP algorithm [40], link the hidden's output to its input. The ability to distribute dynamic information could be improved by using internal feedback. A dynamic mapping function can be created by enhancing the dynamic information, giving the system the ability to adapt time-varying features [42].

A feedforward distributed time delay (FFDTD) neural network was tested next. The FFDTD is a dynamic multi-layered NN that takes into account the temporal properties of the data set [43]. FFDTD-NN uses a series of hidden layers as memory. The delay in time delay NN is only provided to one hidden layer, whereas the delay in FFDTD is provided to all layers, and the FFDTD-NN can also overcome the limitations of shift-invariant [44].

The Nonlinear auto-regressive exogenous network (NARX) was the fifth NN tested in this article. The NARX network, a sort of dynamical NN architecture with multiple layers of feedback connections, is frequently used for input and output modelling of nonlinear dynamical systems [45]. Prediction models based on linear auto-regressive exogenous structures, such as the NARX system, are prevalently used [46]. This model can predict future values of a time series by comparing current values to previous values, as well as current and previous driving series values [47]. The NARX-NN was easily and effectively implemented to univariate time series that required long-term prediction.

The final NN to be tested in this paper is a recurrent neural network (RNN). This is an ANN that implements time series or sequential data [48]. RNNs are commonly used to solve temporal problems such as image captioning, translation, and speech recognition [49]. As a result, it is widely used in applications such as voice search and translation. RNNs, like FF neural networks, improve their learning by using training data. Input and output are characterized by their "memory" of previous inputs [48]. The output of an RNN is dependent on the previous items in the sequence when used instead of a typical NN [48]. Even though future events may help predict the outcome of a sequence, unidirectional RNNs cannot take these into account when making predictions. RNNs are also highlighted by the fact that each layer in the NN employs the same set of parameters [49]. Unlike FF networks, RRNs have a single weight parameter for each node in the network.

According to the findings acquired when using one hidden layer with ten neurons (FFBP, CFD, ELM, FFDTD, NARX, and RNN) training methods to test data collected by the UWOC experiment, the FFBP was adopted in the proposed system due to its superior performance compared to the other ANN training methods, as shown in Figure 4.

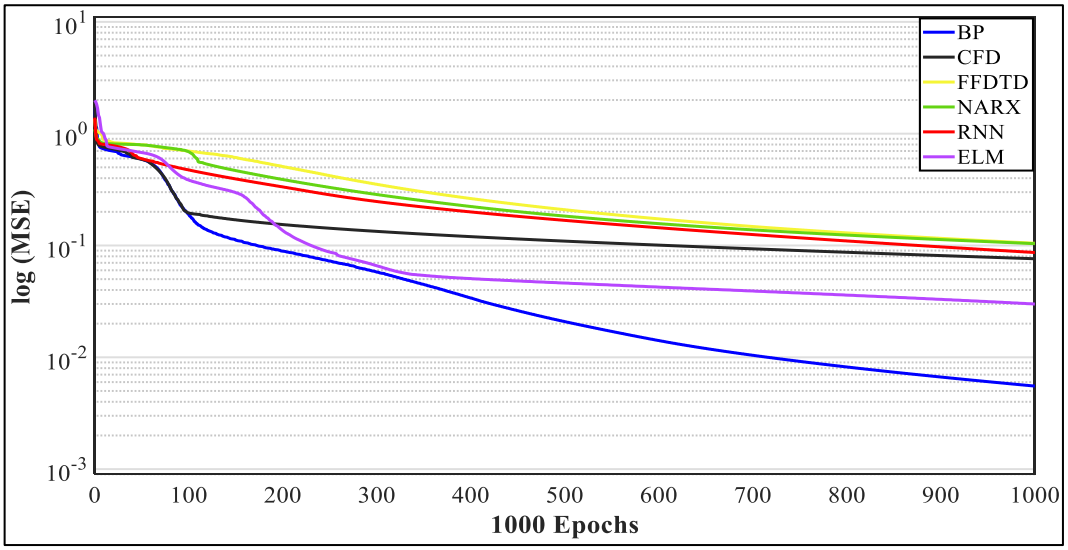

Figure 4: Comparison of different training methods

Figure 4 shows that the mean square error (MSE) of the FFBP-ANN training is (5.3910-3), whereas the MSE of the other training methods ranges between (1.0310-1 and 2.9410-2). As a consequence, the FFBP-ANN was chosen to be used in the proposed OTP control system based on MSE values and to minimize inclusive output errors during the training process. Equation 3 has been used to calculate the MSE values:

$$MSE = \frac{\sum_{i=1}^{n}(\mathcal{P}_e - \mathcal{P}_{ANN})^2}{n} \quad (3)$$

Where *n* is the number of the examined data, $\mathcal{P}_e, \mathcal{P}_{ANN}$ are the transmitted power obtained experimentally and the predicted transmitted power obtained by the proposed ANN model respectively.

4. Results and Discussion

As demonstrated in the preceding section, FFBP-ANN was chosen as the training method for the proposed system. However, the MSE value obtained by one hidden layer of ten neurons falls short of the performance goal in terms of MSE ($1x10^{-3}$) and is insufficient to be used as the final training model. Because the number of neurons in each hidden layer and the rate of learning are the two most significant parameters influencing NN model performance, additional FFBP-ANN models were tested with one hidden layer and (5, 10, 15, 20, 25, 30) neurons, as shown in Figure 5.

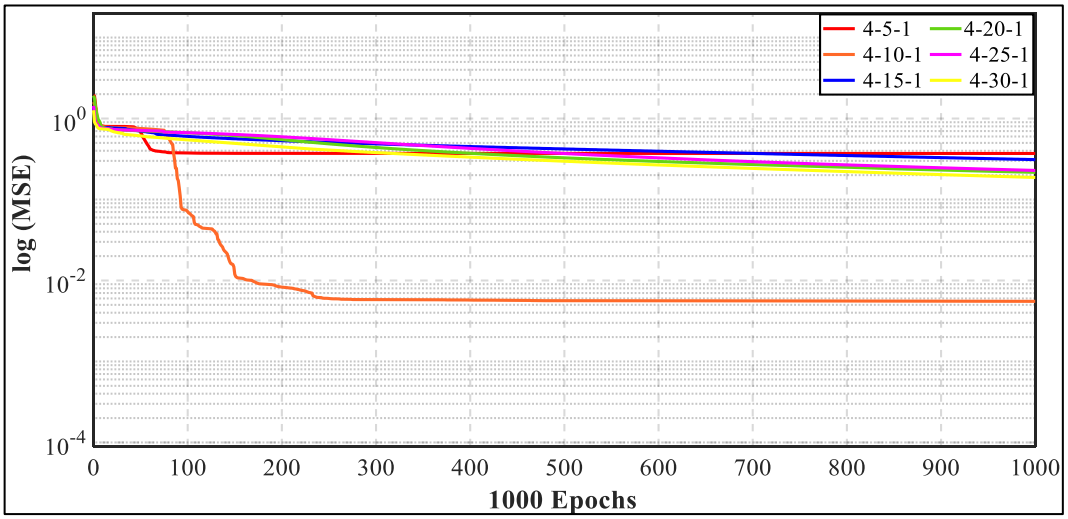

Figure 5: Training performance of FFBP-ANN for one hidden layer and different numbers of neurons

Figure 5 shows that even when the number of neurons is increased to 10, the MSE value of one hidden layer remains the best and fails to meet the performance goal. As a result, another hidden layer was added to the model and tested to achieve better performance than the previous one. The MSE values in Figure 6 are for models with two hidden layers and a number of neurons ranging from 5 to 30, i.e. (5-5,10-10,15-15,20-20,25-25,30-30). As shown in Figure 6, the MSE resulting from the (4-15-15-1) FFBP-ANN model is ($5.6x10^{-4}$), which is the best among the other tested models, despite the fact that there were models with a higher number of neurons. The FFBP-ANN model (4-15-15-1) was used in the current work because it achieved the goal and performed well.

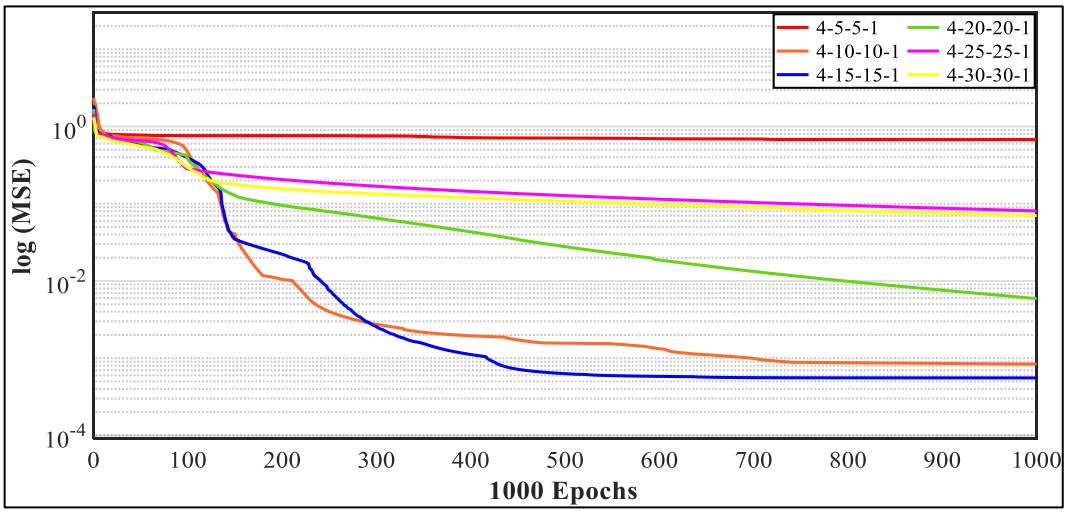

Figure 6: Training performance of FFBP-NN for two hidden layers and different numbers of neurons

Figure 7 depicts the structure of the FFBP-ANN that was used. This model was developed to estimate the best OTP for the actual characteristics of the UWOC channel in order to achieve an acceptable BER. Once the collected data samples were divided into three groups (training, validation, and testing), the training group contained 70% of the samples, while the validation and testing groups contained 30% of the samples split evenly between them.

The adopted FFBP-ANN architecture has four inputs: the distance between transmitter and receiver (D), the primary transmitted power (PTP), the transmitted bit rate per second (Bit/s), and the predicted OTP), fifteen neurons, two hidden layers, and one output layer. To assess the performance of the adopted model, 15% of the collected data samples were tested, and the remaining 15% were validated. Figure 8-a demonstrates the MSE of the predicted OTP for testing samples, and Figure 8-b shows the validation of samples. The proposed ANN model for the UWOC is much more dynamic and less complicated than hybrid acoustic-optical communication-based power-saving and control techniques.

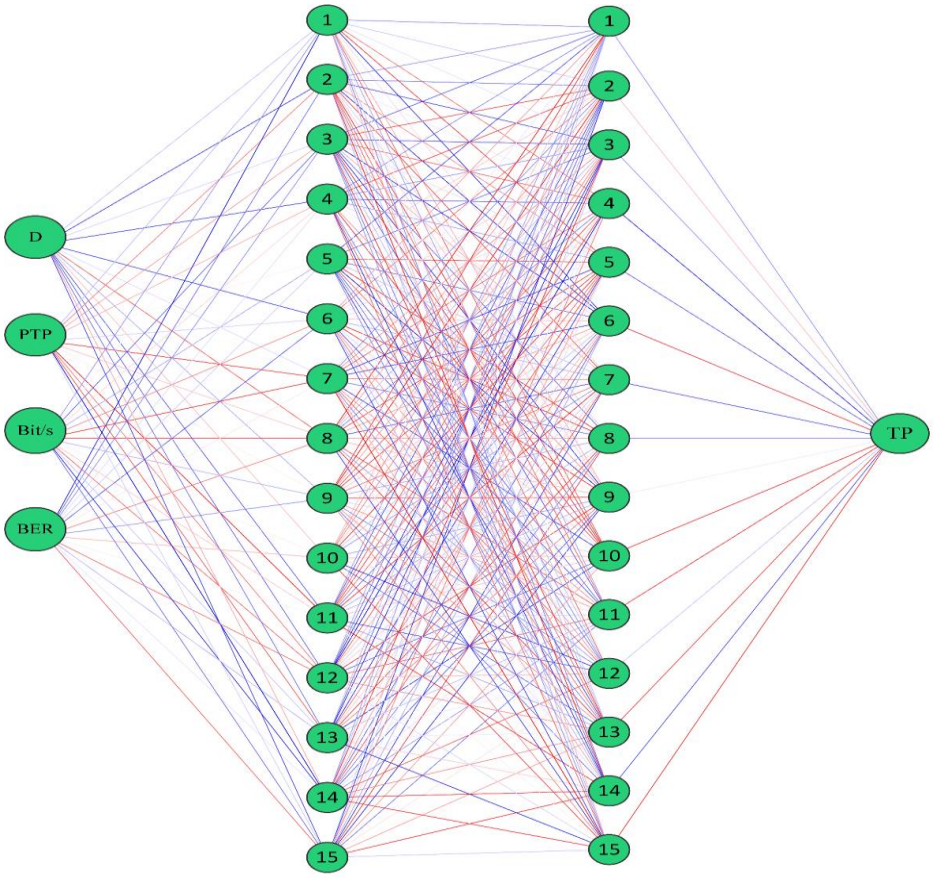

Figure 7: The architecture of the (4-15-15-1) FFBP-ANN

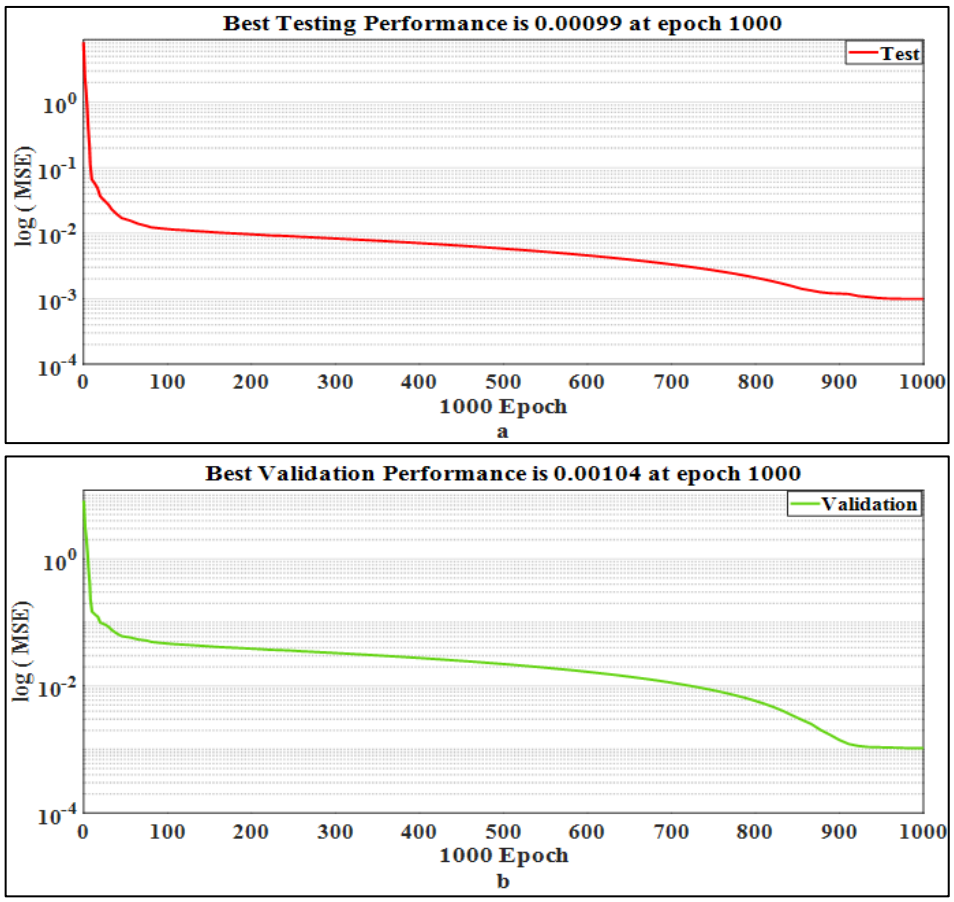

Figure 8: The FFBP-ANN MSE of a) testing and b) validation samples

As could be observed in the testing results and validation samples in Figure 8, 1000 epochs will be adequate to reach the performance goal in terms of the MSE (1 $\times 10^{-3}$). The MSE value for testing is (0.9×10^{-3}) and the MSE value for validation is (1.04×10-3). According to the MSE values, the errors in the predicted OTP when using the proposed model will be (9.5×10^{-3},1.5×10^{-2}, and 1.7×10^{-2}) dBm in the training stage, testing stage, and validation stage.

The proposed evaluation was performed using the quantile-quantile (Q-Q) plot. The Q-Q plots are a helpful visual aid for identifying whether a set of data is consistent with a particular theoretical distribution, such as the Uniform, Normal, or exponential distribution. It is a comparison of practical collected data samples to predicted data samples to see if the two data sets have the same distribution. Figure 9-a depicts the Q-Q plot of the training data samples, Figure 9-b depicts the testing data samples, and Figure 9-c depicts the validation data samples. The Q-Q plot in Figure 9 provides a reliable indication of the proposed system's reliability. R2 values for training, testing, and validation are (0.9997, 0.9990, and 0.9996), which are excellent R2 values in statistical analysis.

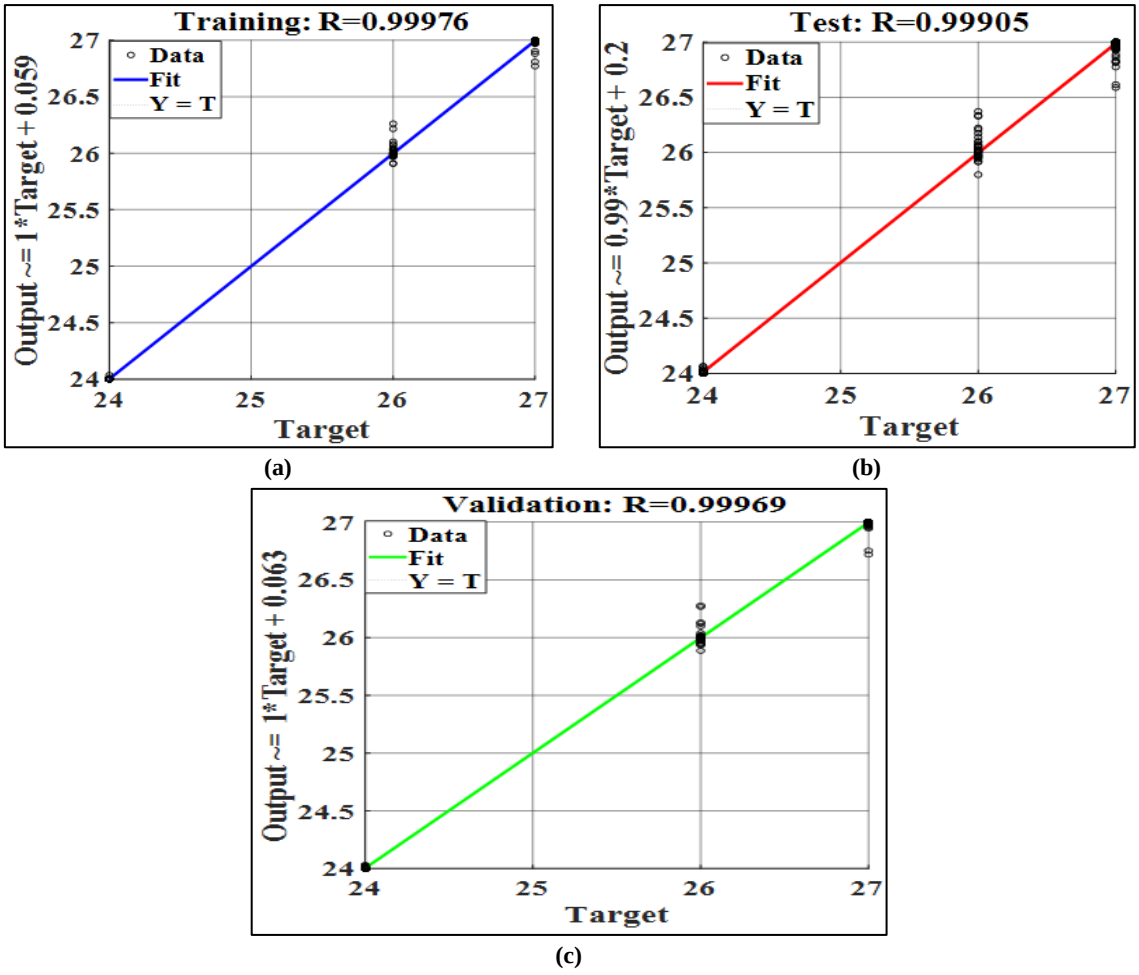

Figure 9: Q-Q plot for a) training b) test and c) validation

5. Conclusion

This work looks into optimizing for low power consumption and reliable data transfer in an underwater environment. Then, for the UWOC system, a dependable ANN model-based transmission power control has been proposed. After testing several well-known algorithms, the FFBP algorithm was chosen to be used for training, testing, and validation of the proposed ANN model because it outperforms the other algorithms tested. Experimentally collected data symbols for the proposed ANN model's training, testing, and validation. In a tank of tap water, a 450 nm laser diode sends (2Mbit/s, 10Mbit/s, and 20Mbit/s) PRBS data. A SiPM sensor receives the transmitted data and analyzes it using a computer. Many scenarios were trialled to fulfil a reliable performance of the proposed FFBP-ANN model by changing the number of neurons and hidden layers. The final FFBP-ANN model that was used consists of two hidden layers, each with fifteen neurons. Where the proposed system model produced a satisfying performance. The proposed ANN model's bitrates of transmitted signals are approximately six times higher than the bitrates of the acoustic-optical system. The proposed ANN model achieves a BER rate that is approximately ten orders of magnitude lower than the hybrid acoustic-optical system. The predicted OTP error in the validation phase is (1.7×10^{-2}) dBm, and in the testing phase is (1.5×10^{-2}), while in the training phase the error in predicted OTP is (9.5×10-3) dBm.

Author Contribution

All authors contributed equally to this work.

Funding

This research received no specific grant from any funding agency in the public, commercial, or not-for-profit sectors.

Data Availability Statement

The data supporting this study's findings are available on request from the corresponding author.

Conflicts of Interest

The authors declare that there is no conflict of interest.

References

[1] H. Zhan, Y. Peng, B. Chen, L. Wang, W. Wang, and S. Zhao, Diffractive deep neural network based adaptive optics scheme for vortex beam in oceanic turbulence, Opt. Express, 30 (2022) 23305. https://doi.org/10.1364/oe.462241

[2] S. A. Adnan, A. Alchalaby, H. A. Hassan, Future Optimization Algorithm to Estimate Attenuation in 532 nm Laser Beam of UWOC-Channel: Improved Neural Network Model, MMEP, 8 (2021) 453–460. https://doi.org/10.18280/MMEP.080316

[3] S. Adnan, M. Ali, and F. Hakwar, The Air Bubbles Effect for Underwater Optical Wireless Communication Using 650 nm Wavelength, Eng. Technol. J., 37 (2019) 398–403. https://doi.org/ 10.30684/etj.37.10a.3

[4] F. Saad, S. A. A. Ibrahim, and M. A. A. Ali, Performance of Underwater Wireless Optical Communication System under Salty Water, IJONS . 9 (2019) 16890–16894. https://doi.org/10.4028/ IJONS.398.29

[5] G. Schirripa Spagnolo, L. Cozzella, and F. Leccese, Underwater Optical Wireless Communications: Overview, Sensors , 20 (2020) 2261. https://doi.org/10.3390/s20082261

[6] S. A. Adnan, H. A. Hassan, A. Alchalaby, and A. C. Kadhim, Experimental study of underwater wireless optical communication from clean water to turbid harbor under various conditions, Int. J. Des. Nat. Ecodynamics, 16 (2021) 219–226. https://doi.org/10.18280/ijdne.160212

[7] Z. Zhou, W. Guan, S. Wen, Recognition and evaluation of constellation diagram using deep learning based on underwater wireless optical communication, arXiv preprint, 2020. https://doi.org/10.48550/arXiv.2007.05890

[8] H. Lu, W. Chen, M. Jiang, Deep Learning Aided Misalignment-Robust Blind Receiver for Underwater Optical Communication, IEEE Wireless Commun. Lett., 10 (2021) 1984–1988. https://doi.org/10.1109/LWC.2021.3089554

[9] C. Gabriel, M. A. Khalighi, S. Bourennane, P. Léon, and V. Rigaud, Monte-Carlo-Based Channel Characterization for Underwater Optical Communication Systems, J. Opt. Commun. Netw., 5 (2013) 1–12. https://doi.org/10.1364/JOCN.5.000001

[10] C. D. Mobley, D. Stramski, W. Paul Bissett, E. Boss, Optical modeling of ocean waters: Is the case 1 - case 2 classification still useful?, Oceanography, 17 (2004) 60–67. https://doi.org/10.5670/OCEANOG.2004.48

[11] S. A. Adnan, M. A. Ali, A. C. Kadhim, M. Sadeq, M. Riaz, Investigating the performance of underwater wireless optical communication with intensity modulation direct detection technique, Opt. Nanostruct. Adv., 71 (2017) 1-3. https://doi.org/10.1364/PV.2017.JW5A.14

[12] C. D. Mobley et al., Comparison of numerical models for computing underwater light fields, Appl. Opt., 32 (1993) 7484–7504. https://doi.org/10.1364/AO.32.007484

[13] Z. Zhou, Z. Peng, J. H. Cui, Z. Shi, Efficient multipath communication for time-critical applications in underwater acoustic sensor networks, IEEE/ACM Trans. Networking, 19 (2011) 28–41. https://doi.org/10.1109/TNET.2010.2055886

[14] S. Han, Y. Noh, R. Liang, R. Chen, Y. J. Cheng, and M. Gerla, Evaluation of underwater optical-acoustic hybrid network, China Commun., 11 (2014) 49–59. https://doi.org/10.1109/CC.2014.6880460

[15] A. Celik, N. Saeed, B. Shihada, T. Y. Al-Naffouri, and M. S. Alouini, A Software-Defined Opto-Acoustic Network Architecture for Internet of Underwater Things, IEEE Commun. Mag., 58 (2020) 88–94. https://doi.org/10.1109/MCOM.001.1900593

[16] H. A. Atiyah, M. Y. Hassan, Outdoor Localization in Mobile Robot with 3D LiDAR Based on Principal Component Analysis and K-Nearest Neighbors Algorithm, Eng. Technol. J., 39 (2021) 965-976. https://doi.org/10.30684/etj.v39i6.2032

[17] H. M. Ahmed and S. R. Hameed, Eye Diseases Classification Using Back Propagation Artificial Neural Network, Eng. Eng. Technol. J., 39 (2021) 11–20. https://doi.org/10.30684/ETJ.V39I1B.1363

[18] O. N. Mohammed Salim, New neuro-fuzzy system-based holey polymer fibers drawing process, AIP Adv., 7 (2017) 105301. https://doi.org/10.1063/1.4998270

[19] Z. Munadhil, S. K. Gharghan, A. H. Mutlag, A. Al-Naji, J. Chahl, Neural Network-Based Alzheimer's Patient Localization for Wireless Sensor Network in an Indoor Environment, IEEE Access, 8 (2020) 150527–150538. https://doi.org/10.1109/ACCESS.2020.3016832

[20] X. Xie, S. Peng, and X. Yang, Deep Learning-Based Signal-To-Noise Ratio Estimation Using Constellation Diagrams, Mob. Inf. Syst., 2020 (2020) 1-9. https://doi.org/ 10.1155/2020/8840340

[21] W. Karner, O. Nemethova, and M. Rupp, Link error prediction in wireless communication systems with quality based power control, IEEE ICC, 2007, 5076–5081. https://doi.org/10.1109/ICC.2007.838

[22] J. Zou, Y. Han, and S. S. So, Overview of artificial neural networks, Methods Mol. Biol., 458 (2008) 15–23. https://doi.org/10/1007/978-1-60327-101-1

[23] J. Schmidhuber, Deep learning in neural networks: An overview, Neural Netw., 61 (2015) 85–117. https://doi.org/0.1016/J.NEUNET.2014.09.003

[24] I. Hameed, P. V. Tuan, and I. Koo, Exploiting a deep neural network for efficient transmit power minimization in a wireless powered communication network, Appl. Sci., 10 (2020) 4622. https://doi.org/10.3390/app10134622

[25] R. Jiao, X. Huang, X. Ma, L. Han, and W. Tian, A Model Combining Stacked Auto Encoder and Back Propagation Algorithm for Short-Term Wind Power Forecasting, IEEE Access, 6 (2018) 17851–17858. https://doi.org/10.1109/ACCESS.2018.2818108

[26] S. R. Devi et al., Performance Comparison of Artificial Neural Network Models for Daily Rainfall Prediction, Mach. Intell. Res., 13 (2016) 417–427. https://doi.org/10.1007/S11633-016-0986-2

[27] R. M. Palnitkar and J. Cannady, A review of adaptive neural networks, IEEE SoutheastCon, 2004. Proceedings., Greensboro, NC, USA, 2004, 38-47. https://doi.org/10.1109/SECON.2004.1287896

[28] R. A. Mohammed, O. N. M. Salim, A. H. Al-Nakkash, and A. A. S. Alabdullah, Proposed APs Distribution Optimization Algorithm: Aware of Interference (APD-AI), IOP Conf. Series Mater. Sci.Eng., 745,2020, 012040. https://doi.org/10.1088/1757-899X/745/1/012040

[29] A. H. Mutlag, O. N. M. Salim, and S. Q. Mahdi, Optimum PID controller for airplane wing tires based on gravitational search algorithm, Bull. Electr. Eng. Inform., 10 (2021)1905–1913. https://doi.org/10.11591/EEI.V10I4.2953

[30] A. H. Mutlag, S. Q. Mahdi, S. K. Gharghan, O. N. M. Salim, A. Al-Naji, and J. Chahl, Improved Control System Based on PSO and ANN for Social Distancing for Patients With COVID-19, IEEE Access, 10 (2022) 63797–63811. https://doi.org/10.1109/ACCESS.2022.3183124

[31] A. H. Mutlag, S. Qays Mahdi, and O. N. Mohammed Salim, A Comparative Study of an Artificial Intelligence-Based Vehicle Airbag Controller, IEEE 18th, CSPA Proceeding, 2022, 85–90. https://doi.org/10.1109/CSPA55076.2022.9782038

[32] A. Malekian and N. Chitsaz, Concepts, procedures, and applications of artificial neural network models in streamflow forecasting, Adv.Streamflow Forecasting, (2021) 115–147. https://doi.org/10.1016/B978-0-12-820673-7.00003-2

[33] A. H. Mutlag, S. Q. Mahdi, and O. N. M. Salim, A New Switching Controller Based Soft Computing-High Accuracy Implementation of Artificial Neural Network, Int. J. Comput. Sci.Commun. Netw., 7 (2017). 01–16.

[34] C. Yang, H. Kim, S. P. Adhikari, and L. O. Chua, A Circuit-Based Neural Network with Hybrid Learning of Backpropagation and Random Weight Change Algorithms, Sensors, 17 (2016) 16. https://doi.org/10.3390/S17010016

[35] H. A. R. Akkar, S. Qasim, and G. Haddad, Diagnosis of Lung Cancer Disease Based on Back-Propagation Artificial Neural Network Algorithm, Eng. Technol. J., 38 (2020) 184–196. https://doi.org/10.30684/ETJ.V38I3B.1666

[36] X. Lin et al., All-optical machine learning using diffractive deep neural networks, Science (1979), 361 (2018) 1004–1008. https://doi.org/10.1126/science.aat8084

[37] I. M. Jaber; H. A. R. Akkar; H. R. Hatem, OFDM Channel Estimation Based on Intelligent Systems, Eng. Technol. J., 32 (2014) 305-324.

[38] N. Farsad and A. Goldsmith, Neural network detection of data sequences in communication systems, IEEE Trans. Signal Process. , 66 (2018) 5663–5678. https://doi.org/10.1109/TSP.2018.2868322

[39] M. Yang, B. Xie, Y. Dou, and G. Xue, Cascade Forward Artificial Neural Network based Behavioral Predicting Approach for the Integrated Satellite-terrestrial Networks, Mobile Netw Appl., 27 (2022) 1569–1577. https://doi.org/10.1007/s11036-021-01875-6

[40] M. M. M. Elshamy, N. T. Artem, V. U. Evgeniya, and M. Z. Elgendy, Comparison of feed-forward, cascade-forward, and Elman algorithms models for determination of the elastic modulus of pavement layers, ACM Series., (2021) 46–53. https://doi.org/10.1145/3465222.3465235

[41] W. Jia, D. Zhao, T. Shen, Y. Tang, and Y. Zhao, Study on optimized Elman neural network classification algorithm based on PLS and CA, Comput. Intell. Neurosci., 2014 (2014)12. https://doi.org/10.1155/2014/724317

[42] G. Ren, Y. Cao, S. Wen, T. Huang, and Z. Zeng, A modified Elman neural network with a new learning rate scheme, Neurocomputing, 286 (2018) 11–18. https://doi.org/10.1016/J.NEUCOM.2018.01.046

[43] A. M. Hemeida et al., Nature-inspired algorithms for feed-forward neural network classifiers: A survey of one decade of research, Ain Shams Eng. J. Ain Shams University, 2020. https://doi.org/10.1016/j.asej.2020.01.007

[44] W. Wang, C. Zhang, W. Wang, and C. Zhang, Bifurcation of a feed forward neural network with delay and application in image contrast enhancement, MBE . 17 (2020)387–403. https://doi.org/10.3934/MBE.2020021

[45] J. M. P. Menezes and G. A. Barreto, Long-term time series prediction with the NARX network: An empirical evaluation, Neurocomputing, 71 (2008) 3335–3343. https://doi.org/10.1016/J.NEUCOM.2008.01.030

[46] H. Xie, H. Tang, and Y. H. Liao, Time series prediction based on narx neural networks: An advanced approach, Proceedings of the 2009 ICMLC, 3 (2009) 1275–1279. https://doi.org/ 10.1109/ICMLC.2009.5212326

[47] Q. Liu, W. Chen, H. Hu, Q. Zhu, and Z. Xie, An Optimal NARX Neural Network Identification Model for a Magnetorheological Damper With Force-Distortion Behavior, Front. Mater., 7 (2020) 10. https://doi.org/10.3389/FMATS.2020.00010/BIBTEX

[48] Robert, R.D, Gregory D.Hager.2020. Deep learning: RNNs and LSTM, Handbook of Medical Image Computing and Computer Assisted Intervention, Vol.21, pp. 503–519. https://doi.org/10.1016/B978-0-12-816176-0.00026-0

[49] A. Lazar, G. Pipa, and J. Triesch, SORN: A self-organizing recurrent neural network, Front. Comput. Neurosci. , 3 (2009) 1-9. https://doi.org/10.3389/NEURO.10.023.2009/BIBTEX